COMPRESSIBILITY MODELING AND VALIDATION FOR COUPLED FLOW SIMULATION

A. George[1]*, H. Ahlborn[2], M. ElGhareeb[2], K. Drechsler[2], D. Heider[3]
[1] Swerea SICOMP, Piteå, Sweden, [2] Institute of Aircraft Design, University of Stuttgart, Stuttgart, Germany, [3] Center for Composite Materials, University of Delaware, Newark, USA
* Corresponding author (andy.george@swerea.se)

Keywords: *Compressibility, Liquid Composite Moulding, Vacuum Infusion, Thickness Gradient, Debulking, Fiber Wetting*

1 Introduction

In simulation of flow under a flexible cover, such as vacuum infusion (VI), the permeability of the fabric is not constant because of thickness changes. Thus, the accuracy of flow simulation can be improved by incorporating both the relationship between permeability and thickness, as well as a model to predict the thickness. The local thickness of the reinforcement during infusion can be related to the fabric compaction pressure (P_C). And the local P_C can be determined when the local pressure on the resin (P_R) is known by:

$$P_{Atmospheric} = P_R + P_C \quad (1)$$

The P_R is a linear gradient along the flow length for resin transfer molding (RTM) via Darcy's Law. For VI, an analytical model for P_R that allows for vacuum bag displacement has been developed [1,2].

Previous attempts at coupling compressibility modeling to flow simulation have reported only 10-20% differences in the predicted fill times, and concluded that the sacrifice of computing time was not worth it due to the high scatter in permeability [1]. But flow simulation is continuing to improve and reduce this scatter. Thus, the importance of compressibility modeling will become of greater importance as accuracy improves.

In this study, a variety of modern advanced carbon preform materials are characterized for their compressibility. The difference of wetting fluids is investigated, to determine how accurate the substitution of epoxy with oil is.

2 Methodology

During VI, a sequence of compactions and expansions occurs in the reinforcement. The dry textile is placed under vacuum and compacted to a high pressure with nesting. This thickness increases behind the flow front as P_R relieves P_C. Once the mould is filled, the inlet is typically either closed or subjected to vacuum to reduce the thickness gradient and remove excess resin. The thickness variation throughout this cycle depends on the location. Previous literature has shown the compressibility's sensitivity to the compressive velocity, history, and magnitude [3], as well as the lubrication [4] of the reinforcement.

Most compression testing is done with a typical tensile testing machine with flat heads. This assumes that the difference in compaction between flat heads and a vacuum bag is minimal [2]. More accurate testing consists of *in-situ* infusions with pressure sensors [2,5], and bag deflection measurement by means such as digital speckle photography [5].

Many compression studies model the P_C as a power law function of the thickness, but this shows poor fitting at high fiber contents (v_F) [2,6]. The model proposed in [4] is tailored to wet expansion modeling and showed excellent fits for modern fabrics [6]:

$$1-\left(\frac{v_{F0}}{v_F}\right)=a+b\left(\frac{P_C}{c+P_C}\right) \quad (2)$$

where v_{F0} is the initial dry v_F of the uncompressed fabric, and a, b, and c are fitting constants.

2.1 Materials

100 mm x 100 mm samples of various reinforcement materials were prepared for pure compression testing. These include carbon non-crimp fabrics (NCF), braids, and tailored fiber placement (TFP) fabrics. These materials are described in [6]. A carbon uni-directional (UD) bindered NCF (242 g/m^2) (16 plies) and a fiberglass chopped strand mat (CSM) (Ahlstrom M601-600) (6 plies) were added to that set of materials for this work.

Both dry and wet samples were tested. Wetting was done by laying the sample in a bath of either rapeseed oil (RO), silicon oil (SO), or epoxy (Huntsman LY556 with no initiator).
The epoxy-wetted samples were placed in an epoxy bath at 50°C. For testing, the cooled samples had a viscosity of ~1000 mPa·s. Another bath was prepared with the same epoxy, but thinned with a small amount of acetone, for a viscosity of ~150 mPa·s. This is much closer to the oils, whose viscosity during testing was 91 (SO) and 59 mPa·s (RO).
Samples were also prepared for infusion under a vacuum bag. The UD-NCF and the glass CSM were each infused with a room temperature curing epoxy (Huntsman LY5052).

2.2 Testing

2.2.1 Pure Compression Characterization

A tensile testing machine was used in compression mode to monitor the stress-strain development. Each sample was compressed at a quick strain rate (1 mm/min) to mimic vacuum application, and then held at 100 kPa (maximum P_C in VI). The constant pressure was maintained over this holding step by continued compression as the sample underwent nesting rearrangement. Once an equilibrium stress-strain was achieved, the sample was then allowed to expand at a slow rate (0.2 mm/min) to mimic resin arrival and further filling. This cycle was then repeated 1 or 2 times, to simulate the industrial practice of debulking to achieve a final high v_F.

2.2.2 Vacuum Bag Deflection Measurement

An ARAMIS camera system was used with digital speckle photography to monitor the vacuum bag deflection during the VI trials. The details of digital speckle photography can be found in [5].

3 Results

3.1 Pure Compression

All sample thicknesses were converted to v_F values. A comparison between the 1st dry expansion and 1st and 2nd wet expansion curves (wetted in RO), and their best power law fits is given in Fig.1 for the UD-NCF. The power law does not adequately describe the high rigidity at high v_F values. As most of the preform is at the highest levels of v_F during infusion, this is the most important degree of compaction for flow modeling. An excellent fit results from (2) for both expansion cycles, as it did for the other materials and fluids.
Fig.1 also illustrates the pressure response difference between dry and wet fabrics. The wet samples show higher v_F's (lubrication). Also seen is the typical viscoelasticity: the 1st wet expansion cycle is shifted to higher v_F's for the 2nd wet expansion cycle.

3.1.1 Carbon NCF-UD

For the UD-NCF, the average expansion curve for three replicates was calculated for each of the four test fluids. These are illustrated in Fig.2 along with their fits to (2). Error bars (very small) represent the standard error at every 10th data point. "TE" and "EP" represent thinned epoxy and the high-viscosity epoxy, respectively. The 2nd cycle curves are shifted to the right for all fluids. Note: no 2nd cycle data is available for "TE."
The RO curves are closer to the epoxy curves than the SO curves. The TE curve is much closer to the oil-wetted curves than the EP curve. It would seem that either the reduced viscosity or a reduced shear due to the acetone's affect on the monomer has made the compressibility behave more like the oils.
The reason for the epoxy's steeper curve (stiffer) compared to the oil-curves is thought to be viscosity related. The high viscosity imparts a shear as the fluid is forced out or drawn back during compression or expansion. The sample may not expand as quickly as the crosshead movement due to the shear. Thus the pressure drops to almost 0 with only a slight movement of the crosshead. Indeed, the TE curve is less steep at low pressures.
But this cannot explain the high starting v_F (at 100 kPa) for wet expansion. It is assumed that all the resin is eventually forced out during the pressure holding step to achieve a similar compaction to the oil-wetted samples. Yet the epoxy curves resulted in significantly higher v_F's than the oil-based tests. The cause for such high v_F's remains unknown. Viscosity cannot be the only determinant of the starting v_F, as SO has a slightly higher viscosity, and yet a lower starting v_F than RO.

3.1.2 Glass CSM

The average for all fluids is also presented for the glass CSM (Fig.3). Less hysteresis is observed between the 1st and 2nd cycles. The RO curves are again slightly closer to the epoxy curves than the SO curves.

A significant effect from changing the viscosity of the epoxy is also seen here. Again, lower viscosity seems to make a more compliant curve.

3.1.2 Other Materials

In previous work [6], several other materials were all tested with SO of twice the viscosity (183 mPa·s compared to 91). The same RO was also used (59 mPa·s) in comparison. While the above results with the low viscosity SO showed slightly lower v_F than RO wetting, the opposite case occurred with all of the tests using the higher viscosity SO. The difference between oils was also greater. The low viscosity SO gave v_F 2 to 3% (absolute) lower than RO. But the high viscosity SO gives fiber contents 5 to 10% higher for these materials. Again, the reason for higher v_F with a higher viscosity cannot be explained at this time.

3.2 Model Evaluation by Cured Thickness

In an attempt to verify which oils' results are more accurate to epoxy filling, both oil models were compared to the measured v_F from experimental infusions. Two VI infusions were made with the UD NCF and epoxy (1000 mPa·s), and cured with the full thickness gradient from inlet to vent. The thickness of the cured laminate was measured by optical microscopy at regular intervals along the flow path. These measurements were corrected for cure shrinkage and then converted to v_F values. These values were then compared to the model predictions for each of the test fluids (Fig.4). Although the infusion was made with epoxy, the oil-based models match the thickness better than the epoxy-based models. Of the two oils, the RO model seems to predict the high compaction areas better.

An epoxy with a viscosity of 245 mPa·s was also infused into some of the other materials. Vacuum pressure of 30 kPa was applied post-filling to both the vent and inlet after infusion (P_C = 70 kPa). The thickness was measured at various locations close to the vent. The resultant v_F was compared to the model for 70 kPa (Fig.5). In all but two materials, the RO model seemed to fit the experiments better.

3.3 Model Evaluation by Bag Displacement

3.3.1 Carbon NCF-UD

A 150 mm x 150 mm UD-NCF sample was infused with epoxy (LY5052) while monitoring the bag deflection. The GOM software package was used to analyze the deflection results from the ARAMIS camera system. Points were chosen at 0, 10, 20, 40, 70, and 140 mm along the flow path which results in displacement vs. time curves (bottom left, Fig.6). The sudden drop of all displacements at 1700s corresponds to the time at which the inlet tube was clamped shut. A line of continuous points along the flow path was also designated, to monitor the displacement along the entire length at any given time (top left, Fig.6). This displacement profile shows the initial negative displacement as the fibers begin to be lubricated and the compressibility model shifts from the dry curve to the wet curve. Moving towards the inlet from there, or advancing the time at that point both result in increasing thickness as P_R begins to alleviate the fiber compaction. The full field displacement is represented in color contours (bottom right, Fig.6).

The flow front position at a given time can be determined by measuring the first point of negative displacement in the deflection profile. A thin strip of tape was place on the vacuum bag before applying the speckle paint, and then removed to leave an un-painted region. This was useful for verifying the flow front position as measured by the deflection profile.

A reference for the starting thickness is required to convert displacement to the thickness for every location and time. During pure compression testing of the dry samples, the thickness at the end of the first compaction was measured and used as this reference.

Once all the part thicknesses are calculated, they can be converted to v_F's. The model developed from pure compression testing was then used to predict P_C for each of those v_F's. P_R can then be determined for every location and time from this and the ambient pressure (1). The P_R profile along the center line was calculated in this way at flow front lengths of 20, 40, 70, 100, and 135 mm. The results are graphed in Fig.7, versus the non-dimensionalized location along the flow path (α = position / length of flow).

Fig.7 also includes three variants of simulated P_R curves. The linear P_R curve for RTM is the solid line. The dashed line is the P_R curve predicted by the compression-coupled analytical model in [2], modified to incorporate (2). The resulting curve of P_R vs. flow length bends towards higher P_R from the linear model. This results in a slightly faster fluid velocity, and thus lower fill time. The dotted line is a

theoretical curve coupling a model for capillary pressure (P_{cap}) to the compressibility and flow. It augments the available pressure gradient at the flow front by P_{cap}. The model details are presented in [6].

The RO wet expansion model was used as the SO model under predicts P_R (all reach $P_R = 0$ at $\alpha = 0.3$ to 0.45), and the epoxy models over predict P_R (P_R almost never below 80 kPa). Despite this being an epoxy infusion, the RO model gives the most sensible pressure predictions. The viscosity for the epoxy infusion was around 1000 mPa·s, and even higher at the infusion end due to curing. This is 17 times the viscosity of RO. Thus similar viscosities are not required for a good fit.

Previous work produced similar P_R profiles for infusions monitored not by bag displacement, but by an extensive array of pressure sensors [2]. Their work showed that the bent P_R profile predicted by compressibility models is only achieved at high flow lengths. Before that, the full pressure gradient from ambient to vacuum has not developed yet, and the P_R profile actually sags to lower pressures. This can be seen in Fig.7 as well. For low front lengths, especially the 40 mm flow front, P_R sags below the linear profile. But for later filling lengths, the profile moves upwards to resemble the predicted compressibility-coupled curve.

But there are two significant deviations in this graph from those shown in [2]. First, there are "tails" at the end of each P_R profile, corresponding to the region where the fabric is only partially wetted, and is moving from the dry compressibility behavior to the wet one. Thus, the fully-saturated wet model cannot give accurate pressure predictions for the given thicknesses in that region. These tails can be used, however, to show the length of the partially-wetted region. As the flow length increases, this region becomes shorter in relation to the total flow length, and the tail becomes a smaller portion of α. This could be useful, for example, to measure the difference in time between resin first reaching the outlet and complete filling of the part.

The other significant deviation is the drop in P_R at the end of the long front lengths. Beginning with the 70 mm length, the P_R profile begins to droop at around $\alpha = 0.45$. The 135 mm length profile seems to begin drooping earlier, at about $\alpha = 0.3$, and drops very strongly, to a negative P_R long before it gets to $\alpha = 1$. This sagging is suspected to be due to P_{cap} forces, which only become significant at low fluid velocities. Modern highly-oriented fabrics such as this one have low permeabilities and are generally not infused without the help of an in-plane flow. But in this case, the flow velocity is unaided and becomes very low as the epoxy viscosity rises. The flow-rate eventually drops to a slower speed than the intra-tow flow caused by capillary draw. The capillary forces then become an aid to the macro flow, by "pulling it along." This scenario along with the same sagging profile was suggested in [6]. But there were no experimental results to validate such a drooped curve until now. The dotted line represents the P_R profile for the infusion, with a rough estimate for viscosity build-up, the rapeseed compressibility model, and best guesses for P_{cap} model variables. It shows the same trend as experiment: initially following the compressibility bent curve, and then dropping to a negative P_R.

It is not yet understood what a negative P_R can represent. It is thought to actually be the driving pressure for flow, being the sum of a very low P_R and a P_{cap} modification. Further characterization work is planned, using pressure sensors along the mold, and characterization of P_{cap} variables for this reinforcement and resin.

The good fit of the epoxy model from the testing machine to a VI infusion seems to imply that RO data from flat heads can indeed be applied to VI with negligible error. The high v_F's seen for EP data in Fig.2 do not carry over to the actual epoxy infusion, however. A similar infusion with RO showed bag deflection nearly equal to that of the epoxy infusion. An infusion with SO showed slightly higher bag displacement (representing lower v_F's) than for RO or epoxy. This agrees at least with the slight shift to the left in Fig.3 for the SO curves compared to RO.

3.3.2 Glass NCF-UD

The same procedure was repeated for a 200 mm x 150 mm glass CSM sample (Fig.8). In this case, the glass CSM's thinned-epoxy model resulted in the best fit, and is the one presented in Fig.8. The RO model gives similar results, but only when the dry compacted v_F is dropped from the measured value of 32% to 26%, thus increasing all the calculated thicknesses. This value is difficult to measure, and thus could be the cause of the RO model's lesser fit in this one instance.

A similar infusion with RO showed nearly identical bag deflection. This again shows that the actual infusion compressibility does not differ between epoxy and RO nearly as much as it did in the pure compression testing (Fig.3).
The high compliance of the glass CSM is seen in the high curvature of the compressibility model (dotted line) compared to the carbon NCF-UD. The partially saturated region seems to be very long for the glass material. The "tails" account for most of the flow length for flow fronts at 30 and 60 mm. The flow velocities seem fast enough that little sag is seen other than at the longest flow length and highest α.

3.4 Fill time comparison

1-D flow simulations using the compressibility coupled model in [2] were performed on several of the materials, using the RO compressibility models, and permeability data from previous work [6]. The VI model, with steeper pressure gradients at the flow front, always results in shorter fill times. The % decrease in fill time, when switching from the RTM model to the VI model, for various materials is presented in Fig.9, for both flow along the warp (0°) and weft (90°), assuming a pressure gradient of 100 kPa.
Apart from three of the materials the change is less than 20% as mentioned earlier for previous work. But these results suggest the high importance of modeling the compressibility for highly compliant materials like the glass CSM.

4 Conclusions

Fluid choice seems significant in pure compression response. An increase in viscosity seems to always shift the compressibility curves to higher v_F. The mechanism behind this is yet unknown. In actual infusions, the compressibility differences between epoxy and oils have shown to be very small.
Testing with flat heads and rapeseed oil seems to predict well the compressive behavior of VI processing with epoxy. Silicone oil testing seems to cause slightly lower or higher lubrication compared to epoxy / rapeseed oil, depending on the viscosity.
Shear and viscous forces may have affected the epoxy pure compression data; it does not correlate to infusion thicknesses as well as the oil-based data does. Until these differences can be accounted for, oil-wetted testing is the only recommended method to produce compressibility data outside of an actual infusion.
The measurement of bag deflection during VI has successfully been correlated to pressure profiles matching flow simulation models. A drop in resin pressure seen at slow flows is suspected to be caused by capillary pressure.

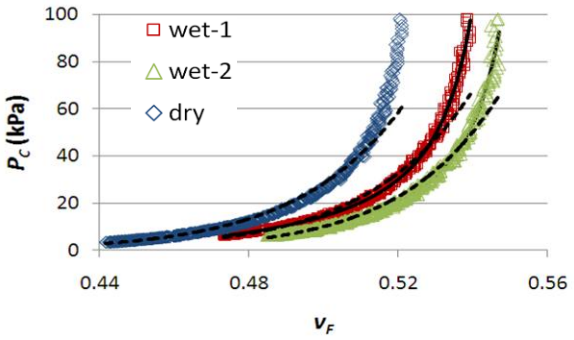

Fig.1. Expansion: 1st dry, 1st wet, and 2nd wet. Fits to (2) (solid lines) and power law (dashed lines).

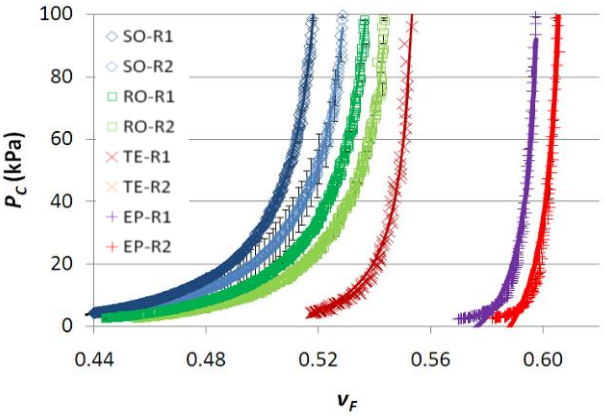

Fig.2. Carbon NCF-UD compression results and fits.

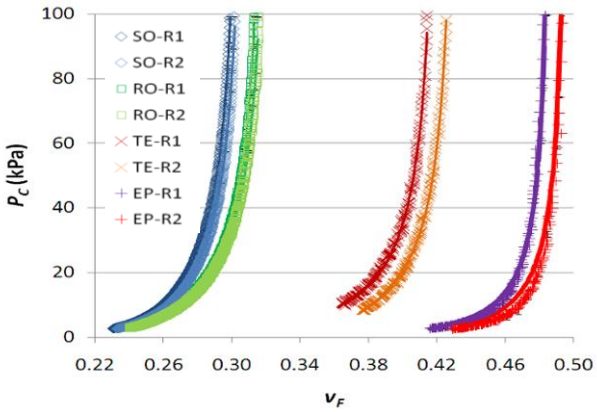

Fig.3. Glass CSM compression results and fits.

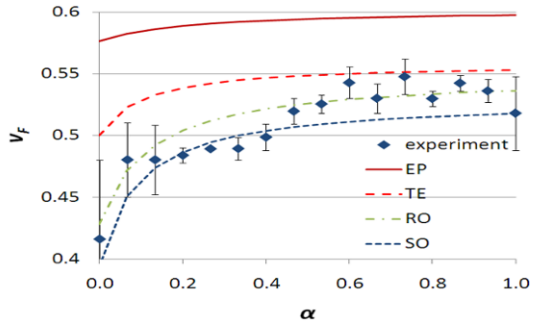

Fig.4. Measured cured thickness vs. models.

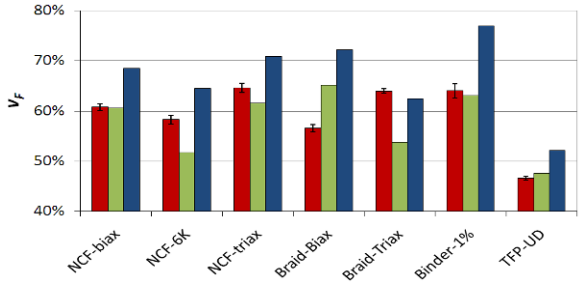

Fig.5. v_F at 70 kPa: experimental (left), RO model (center), SO model (right).

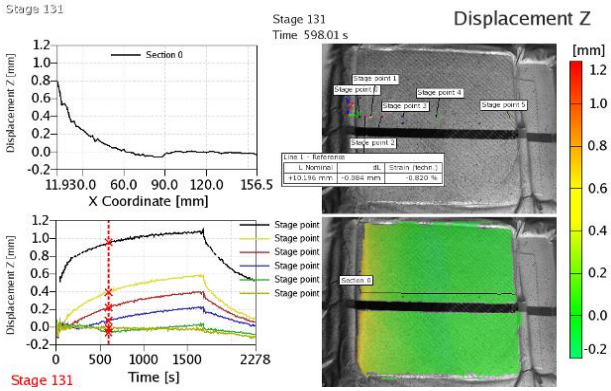

Fig.6. Bag displacement results for carbon NCF-UD.

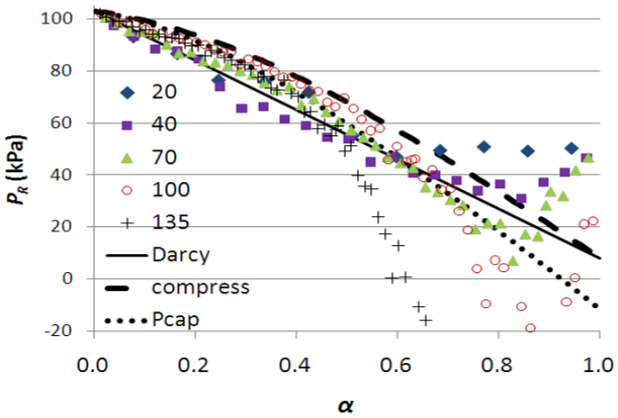

Fig.7. NCF-UD: calculated P_R at various flow lengths vs. prediction.

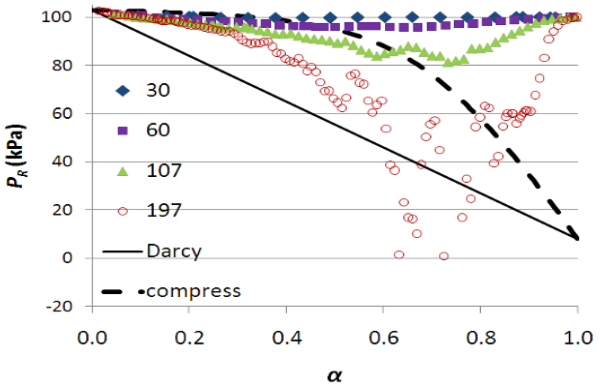

Fig.8. Glass CSM: calculated P_R at various flow lengths vs. prediction.

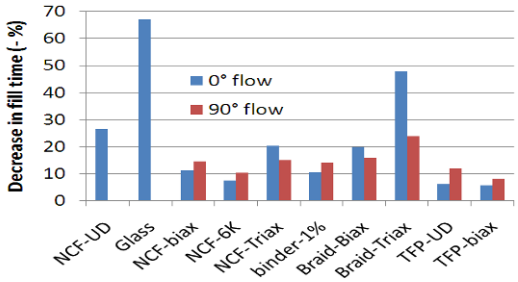

Fig.9. Change in fill time from RTM to VI model.

References

[1] N. Correia "*Analysis of the vacuum infusion moulding process*". PhD. thesis, University of Nottingham, 2004.

[2] D. Modi "*Modeling and Active Control of the Vacuum Infusion Process for Composites Manufacture*". PhD. thesis, University of Nottingham, 2008.

[3] F. Robitaille, and R. Gauvin "Compaction of textile reinforcements for composites manufacturing. III. Reorganization of the fiber network". *Polymer Composites*, Vol. 20, No. 1, pp 48-61, 1999

[4] B. Grimsley "*Characterization of the Vacuum Assisted Resin Transfer Molding Process for Fabrication of Aerospace Composites*". M.Sc. thesis, Virginia Polytechnic Institute and State University, 2005.

[5] Q. Govignon, et al. "Full field monitoring of the resin flow and laminate properties during the resin infusion process". *Composites: Part A*, Vol. 39, pp. 1412–1426, 2008.

[6] A. George "*Optimization of Resin Infusion Processing for Composite Materials*". PhD. thesis, University of Stuttgart, 2011.